ЖЭТФ, 2008, том 133, вып. 1, стр. 162–170

FLEXIBLE-TO-SEMIFLEXIBLE CHAIN CROSSOVER ON THE PRESSURE–AREA ISOTHERM OF A LIPID BILAYER

I. N. Krivonos, S. I. Mukhin*

Moscow Institute for Steel and Alloys
119049, Moscow, Russian Federation

Received June 11, 2007

We find theoretically that competition between $\sim K_f q^4$ and $\sim Qq^2$ terms in the Fourier-transformed conformational energy of a single lipid chain, in combination with interchain entropic repulsion in the hydrophobic part of the lipid (bi)layer, may cause a crossover on the bilayer pressure–area isotherm $P(A) \sim (A - A_0)^{-\alpha}$. The crossover manifests itself in the transition from $\alpha = 5/3$ to $\alpha = 3$. Our microscopic model represents a single lipid molecule as a worm-like chain with a finite irreducible cross-section area A_0, a flexural rigidity K_f, and a stretching modulus Q in a parabolic potential with the self-consistent curvature $B(A)$ formed by entropic interactions between hydrocarbon chains in the lipid layer. The crossover area A^* obeys the relation $Q/\sqrt{K_f B(A^*)} \approx 2$. We predict a peculiar possibility of deducing the effective elastic moduli K_f and Q of an individual hydrocarbon chain from the analysis of the isotherm with such a crossover. Also calculated is crossover-related behavior of the area compressibility modulus K_A, the equilibrium area per lipid A_t, and the chain order parameter $S(\theta)$.

PACS: 87.16.Dg, 87.15.Kg, 31.15.Kb

1. INTRODUCTION

Studying thermodynamics of lipid bilayers that form biological membranes is of fundamental interest for understanding the relation between the membrane state and the functioning of integral membrane proteins [1–3]. The latter are of vital importance for many processes in living cells. Experimental data in lipid membranes indicate the presence of a crossover in the pressure–area isotherms $P(A) \sim (A-A_0)^{-\alpha}$ [4, 5]. Formally, this means that the exponent α changes substantially within some finite interval along the area axis A. A substantial amount of theoretical work has been devoted to the description of the thermodynamic properties of lipid layers including pressure–area isotherms, the chain order parameter as a function of temperature, specific heat, etc. Theoretical approaches range from phenomenological Landau–de Gennes theory [6] to surface equations of states involving clustering [7–10] and raft formation [11]. Molecular dynamics [12] and Monte Carlo simulations [13] have also been used. Besides, the models were considered with a phase transition due to a change in the number of gauche conformations of the hydrocarbon chains [14–20], as well as models focused on the role of the excluded-volume interactions between the chains [21, 22]. These factors were also combined in the form of an additive area-dependent contributions to the surface pressure [20].

In the previous work [23], a theoretical method was proposed for calculating the thermodynamic characteristics of a lipid bilayer starting from a "microscopic" model of a smectic array of semi-flexible finite-length strings with a given flexural rigidity (see Fig. 1). The string is an idealized model of the hydrocarbon chain. The entropic repulsion between the neighboring chains in a lipid membrane is modeled with an effective potential. This entropic potential is then found self-consistently, by minimizing the free energy of the bilayer, which is in turn calculated using path integration over possible conformations of the strings. As a result, the lateral pressure profile inside the lipid bilayer was derived analytically, together with the area compressibility modulus and the temperature coefficient of area expansion of the membrane.

In [23], only the bending energy of strings and the entropic repulsion were included in the conformational

*E-mail: sergeimoscow@online.ru

energy functional. In the Fourier-transformed representation, the bending energy is proportional to $\sim K_f q^4$, where q is the wave vector along the chain axis and K_f is the chain flexural rigidity modulus. The resulting pressure–area isotherm of the lipid bilayer was derived in the form of a power law $P_t(A) \sim (A - A_0)^{-\alpha}$, with the constant exponent $\alpha = 5/3$. The lateral pressure of the lipid hydrocarbon chains (tails) $P_t(A)$ is here expressed as a function of the area per lipid A in the layer at a given temperature, with A_0 being the chain incompressible cross-section area. In the present work, we add the stretching energy of the string to the energy functional [24]. In the Fourier-transformed representation, this energy is proportional to $\sim Qq^2$, where Q is the chain stretching modulus. Hence, our new chain energy functional contains the sum $K_f q^4 + Qq^2 + B(A)$, where $B(A)$ is the self-consistently determined curvature of a parabolic effective entropic repulsive potential felt by a single chain due to surrounding chains in the lipid layer. The bending (flexural) energy dominates at large wave vectors q, while the stretching energy dominates in the small-q limit. The entropic repulsion term $B(A)$ sets an upper limit for the wave vectors q that are essential for thermodynamics. The entropic repulsion increases as the area per lipid in the layer decreases, i.e., the parameter $B(A)$ becomes greater as $A \to A_0$, making the large q important. As a result, the bending energy term $\sim K_f q^4$ dominates, and we recover the pressure–area isotherm in [23] with the exponent $\alpha = 5/3$. On the other hand, when the area per lipid increases, the entropic repulsion becomes weaker, and the parameter $B(A)$ becomes smaller. Hence, the important q also become smaller and the stretching energy term $\sim Qq^2$ dominates. As a result, a new exponent arises [24]: $\alpha = 3$, corresponding to the stretching-dominated conformational energy of the strings (Figs. 2 and 3). This limit value of the exponent is in agreement with the result in [25], where it was derived using a polymer entropy model (harmonic regime) for lipid bilayer surface pressure and confirmed with bilayer elasticity measurements.

We find that the crossover between the two area-per-lipid regions with different values of the exponent α occurs at the area per lipid A^* determined from the condition $Q/\sqrt{K_f B(A^*)} \approx 2$. The physical states of the lipid layer in the two regions separated by crossover differ by a substantial change in the value of the chain order parameter, which characterizes deviations of the chain from the straight line (see Fig. 7). Also calculated are elastic moduli of the membrane and their dependences on temperature and on the microscopic elastic moduli of the individual chains constituting the lipid bilayer (see Figs. 4–6). Finally, we discuss how the fitting of experimental isotherms of lipid bilayers to our theoretical isotherms may help to deduce the elastic moduli K_f and Q of individual lipid chains constituting the membrane.

The plan of the paper is as follows. In Sec. 2, we formulate the physical model [24] of a bilayer and review the path-integral method of summation over all conformations of an idealized hydrocarbon chain [23]. In Sec. 3, we derive and analytically solve (in two different limits) a self-consistency equation for the curvature $B(A)$ of the effective parabolic entropic potential in the layer. The pressure–area isotherms are then derived in analytic form. In Secs. 4–6, we present the results of calculations of the thermodynamic and elastic characteristics of the whole bilayer that follow from our microscopic model. In the Conclusions, we discuss the correspondence of the theoretical results with available experimental data, and consider the applicability region of the approximations that we use.

2. ENERGY FUNCTIONAL OF A LIPID LAYER: THE STRING MODEL

A hydrocarbon chain (see Fig. 1) is modeled as a flexible string with the flexural rigidity K_f and stretching modulus Q; entropic repulsion from surrounding lipid chains is modeled via a parabolic potential with the self-consistently determined curvature $B(= B(A))$:

$$E = \int_0^L \left(K_f \left(\frac{d^2\mathbf{R}}{dz^2} \right)^2 + Q \left(\frac{d\mathbf{R}}{dz} \right)^2 + B\mathbf{R}^2 \right) dz, \quad (1)$$

where L is the chain length. We consider only small deviations of the chains from a straight line: $|\mathbf{R}(z)| \ll L$. This condition is satisfied if

$$\frac{\sqrt{\langle \mathbf{R}^2(z) \rangle}}{L} \leq \left(\frac{k_B T}{L^2 P_{eff}} \right)^{1/2} \ll 1,$$

where P_{eff} is the effective tension in the bilayer and k_B is the Boltzmann constant. The returning force $-B\mathbf{R}(z)$ acts against the deviation $\mathbf{R}(z)$ of the chain from the vertical straight line, where the coordinate z measures the depth inside the lipid layer with the hydrophilic (polar) heads residing at the layer surface $z = 0$, while hydrophobic (nonpolar) tails formed from hydrocarbon chains constitute the body of the slab $0 < z \leq L$. Here, $\mathbf{R}(z)$ is the vector in the xy plane characterizing the deviation from the z axis: $\mathbf{R}^2(z) = X^2(z) + Y^2(z)$.

The energy of a single string therefore consists of three parts: bending, stretching and effective entropic

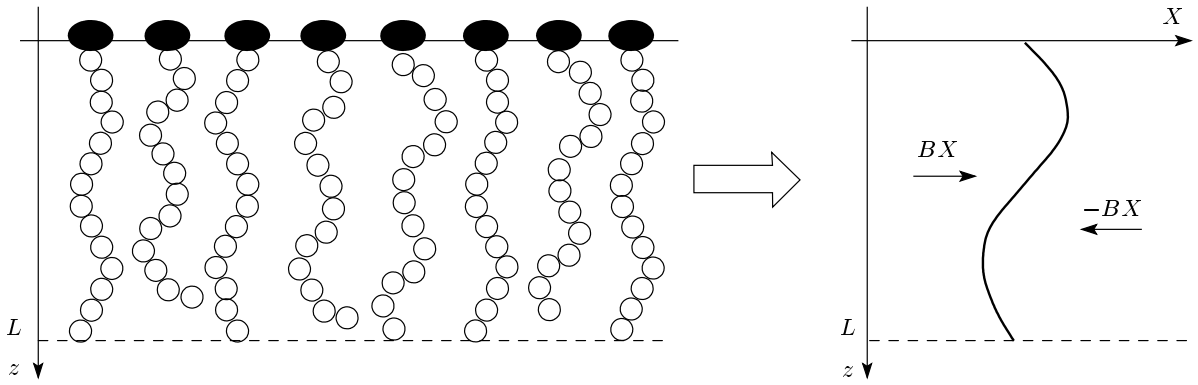

Fig. 1. The model of a lipid membrane in the mean-field approximation. Left panel: sketch of the lipid monolayer (the mirror-symmetric part of the bilayer is not shown). Hydrocarbon tails of lipid molecules form the hydrophobic part of the lipid monolayer. Hydrophilic polar heads (filled ellipses) form the hydrophobic–hydrophilic interface. Right panel: the mean-field flexible-string model of a hydrophobic layer. The arrows indicate entropic forces $\pm BX$ acting on the hydrocarbon chain in the self-consistent entropic potential BX^2, which arises due to surrounding neighbors

potential energies. In equilibrium, the effect of the entropic repulsion is compensated by the interchain attraction due to van der Waals interactions and by the surface tension energy γA, where γ is the surface tension at the hydrophobic–hydrophilic interface [4]:

$$P_t\left(A(T)\right) = P_{eff} = \gamma + P_{hg} + P_{vdW},$$

where $A(T)$ is the equilibrium area per lipid at a given temperature. The total tension in the bilayer is zero. The integral

$$P_t = \int_0^L \Pi_t(z)\, dz$$

of the repulsive (chain) part of the lateral pressure profile $\Pi_t(z)$ over the bilayer hydrophobic region is equal to the balancing effective tension in the bilayer P_{eff}, which, besides the surface tension γ, includes the head group repulsion of electrostatic origin P_{hg}, the pressure arising from van der Waals interactions between chains P_{vdW}, etc. We choose $P_{eff} = 100$ dyn/cm $> \gamma \sim 50$ dyn/cm, because attractive dispersion interactions between hydrocarbon chains are included in the effective surface tension [26]. In general, at room temperature, the effective surface tension for a typical lipid bilayer is in the range $50 \le P_{eff} \le 150$ dyn/cm [2, 26]. Considering a single chain consisting of N links of equal length a for simplicity, we rewrite Fourier-transformed energy functional (1) as

$$E = L^2 \int_{-\pi/a}^{\pi/a} |\mathbf{R}_q|^2 (K_f q^4 + Q q^2 + B) \frac{dq}{2\pi} = L \sum_q |\mathbf{R}_q|^2 E_q, \quad (2)$$

where summation over the wave vector q ranges the interval $2\pi/a$ with the step $2\pi/L$, $E_q = K_f q^4 + Q q^2 + B$, and $\mathbf{R}_q$ is the Fourier transform of the function $\mathbf{R}\,(z)$. Because we consider the membrane that is isotropic in the xy plane, the x- and y-components of the vector field $\mathbf{R}(z)$ make equal contributions to the partition function of the string, and therefore

$$Z = Z_x Z_y = Z_x^2 = \left(\prod_q \int_0^\infty \exp\left(-\frac{L E_q}{k_B T} |X_q|^2 \right) |X_q| d |X_q| \right)^2 = \left(\prod_q \frac{k_B T}{2 L E_q} \right)^2. \quad (3)$$

The free energy $F = -k_B T \ln Z$ can then be expressed as

$$\Delta F = F(B) - F(B=0) = 2 k_B T \sum_q \ln \frac{E_q}{E_q(B=0)}, \quad (4)$$

where the free energy of a free single chain is subtracted for the convergence of the sum.

3. PRESSURE–AREA ISOTHERM OF THE LIPID LAYER EXPRESSED THROUGH THE CURVATURE OF THE INTER-CHAIN ENTROPIC POTENTIAL

The self-consistent equation for the curvature B of the parabolic potential modeling the interchain entropic repulsion in the lipid layer takes the form

$$\frac{\partial F}{\partial B} = 2k_BT\sum_q \frac{1}{E_q} = \langle \mathbf{R}^2\rangle L = \\ = \frac{\left(\sqrt{A}-\sqrt{A_0}\right)^2}{\pi} L, \quad (5)$$

where $A_0 = V_0/L$ is the incompressible area of the chain cross section, V_0 is the incompressible volume of the lipid chain, and $\left(\sqrt{A}-\sqrt{A_0}\right)^2$ is the area swept by the string formed by the centers of the chain cross sections. Obviously, when the area per lipid A is close to the incompressible area A_0, the self-consistent curvature B is large, and we can therefore pass from summation to the integration over the wave vector q in Eq. (5):

$$\left(\sqrt{A}-\sqrt{A_0}\right)^2 = k_BT\int\limits_{-\pi/a}^{\pi/a}\frac{dq}{E_q}. \quad (6)$$

The resulting self-consistency equation for the curvature B is

$$\left(\sqrt{A}-\sqrt{A_0}\right)^2 = \\ = \frac{\pi}{\sqrt{2}}\frac{k_BT}{K_f^{1/4}B^{3/4}}\left(1+\frac{Q}{2\sqrt{BK_f}}\right)^{-1/2}. \quad (7)$$

This equation is solved numerically, but analytic results can also be obtained in the two limit cases: $\xi \ll 1$ and $\xi \gg 1$, where $\xi \equiv Q/2\sqrt{BK_f}$. These two limits respectively correspond to the domination of the bending energy and of the stretching energy:

$$B(A) = \frac{1}{K_f^{1/3}}\frac{\pi^{4/3}(k_BT)^{4/3}}{\sqrt[3]{4}}\left(\sqrt{A}-\sqrt{A_0}\right)^{-8/3}, \quad \xi \ll 1, \quad (8)$$

$$B(A) = \frac{\pi^2(k_BT)^2}{Q}\left(\sqrt{A}-\sqrt{A_0}\right)^{-4}, \quad \xi \gg 1. \quad (9)$$

Relation (8) coincides with the result in Eq. (A.5) in [23], which was obtained by a more detailed method without using the Fourier-transformed version of energy functional (2) and without taking the stretching energy into account. As long as $\xi = \xi(A)$, due to the dependence of the curvature $B = B(A)$ on the area A, the crossover from limit expression (8) to limit expression (9) may occur at some particular area per lipid A^* determined from the condition $\xi(A^*) \approx 1$. This crossover area A^* is found below (see Eq. (14)).

Substituting the self-consistent solution $B = B(A)$ in chain free energy (4), we find the lateral pressure–area-per-lipid isotherm for the hydrophobic part of the lipid (bi)layer:

$$P_t \equiv -\frac{\partial \Delta F(A)}{\partial A} = \frac{\partial B}{\partial A}\sum_q \frac{2k_BT}{E_q}. \quad (10)$$

Because the sum in the right hand side of Eq. (10) also enters self-consistency equation (5), the pressure–area isotherm can be expressed in the closed analytic form

$$P_t(A) = \pi^{-1}\left(\sqrt{A}-\sqrt{A_0}\right)^2 L\frac{\partial B(A)}{\partial A} \quad (11)$$

with the curvature $B(A)$ directly involved.

4. CROSSOVER ON THE LIPID LAYER ISOTHERM: COMMUNICATION BETWEEN "MACRO" AND "MICRO"

It is remarkable that crossover in the isotherm of a lipid (bi)layer in principle provides an intriguing possibility to follow the link between macro- and microscopic properties of the biomembrane. Namely, it is possible to deduce the effective elastic moduli of the individual lipid chains constituting the bilayer from the pressure–area isotherm of the entire macroscopic system.

To explain the deduction "recipe" (see Eqs. (15) and (16) below), we consider theoretical predictions following from the general model described in the previous section. First, we successively substitute Eqs. (8) and (9) in general equation (11) and (in the limit of small enough areas per lipid, $A/A_0 \approx 1$) find analytic formulas describing the lateral pressure–area isotherms of the lipid layer:

$$\frac{P_t}{k_BT} = \frac{2}{3}\left(\frac{\pi k_BT}{4K_f}\right)^{1/3} \times \\ \times VA^{-3/2}\left(\sqrt{A}-\sqrt{A_0}\right)^{-5/3}, \quad \xi \ll 1, \quad (12)$$

$$\frac{P_t}{k_BT} = \frac{2\pi k_BT}{Q} \times \\ \times VA^{-3/2}\left(\sqrt{A}-\sqrt{A_0}\right)^{-3}, \quad \xi \gg 1, \quad (13)$$

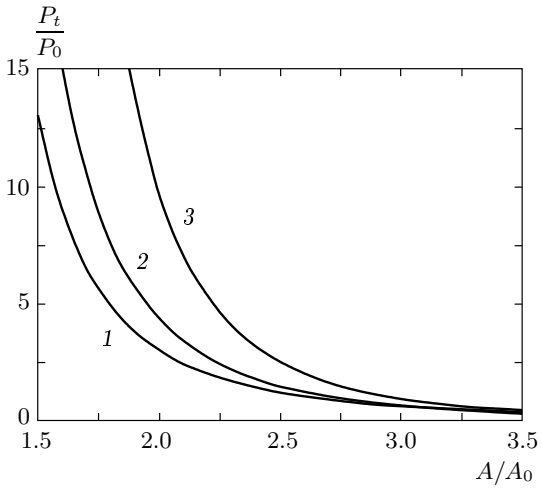

Fig. 2. The calculated pressure–area-per-lipid isotherms for the lateral pressure P_t in the hydrophobic (tails) part of the lipid bilayer with different relative strengths of the single-chain stretching and bending energies characterized by the dimensionless parameter $\sigma = QL^2/K_f$. Isotherm *1* ($\sigma \to 0$) corresponds to the dominating bending energy of the chains (see Eq. (12)); curve *3* ($\sigma \to \infty$) corresponds to the dominating stretching energy of the chains (see Eq. (13)). Curve *2* ($\sigma \approx 10^2$) corresponds to an intermediate case and shows a crossover between the two isotherms drawn in the two limits. A_0 is the incompressible area of the hydrocarbon chain. The temperature for all the curves is $T = 300$ K

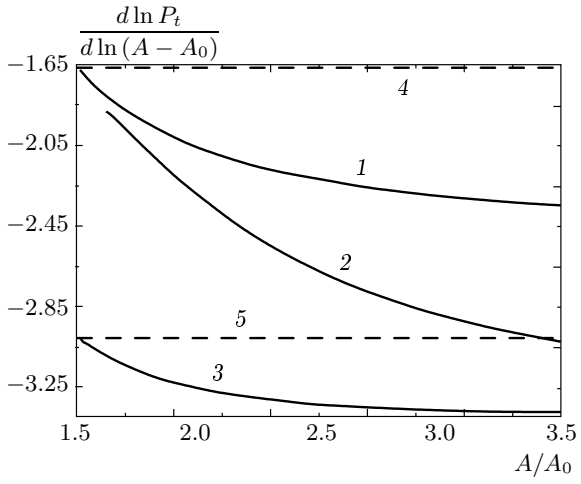

Fig. 3. The same cases as in Fig. 2, but for the calculated logarithmic derivative of the lateral pressure with respect to the area per lipid. The logarithmic derivative gives the value of the exponent $-\alpha(A)$ in the limit $A \to A_0$ in the isotherm equation of state of the lipid bilayer: $P_t \sim (A - A_0)^{-\alpha(T)}$. Curve *2* ($\sigma \approx 10^2$) demonstrates a crossover between the exponents $\alpha = 5/3$ (*4*) and $\alpha = 3$ (*5*) that are shown with straight dashed lines. The other two curves are the exact dependences given by Eqs. (12) and (13) describing the isotherms in the respective limits of the dominant bending (*1*, $\sigma \to 0$) and stretching (*2*, $\sigma \to \infty$) energy of the hydrocarbon chains. The temperature for all the curves is $T = 300$ K

where $V = AZ_m \approx AL$ is the (conserved) volume per lipid molecule in the hydrophobic part of the lipid layer, Z_m is the actual thickness of the hydrophobic part of the lipid layer, and $Z_m \approx L$ in the limit of small deviations from the straight line of the string modeling the chain. Asymptotic relation (12), which is valid for the bending-dominated free energy, is the same as in [23], but relation (13) is new and corresponds to domination of the stretching energy. The crossover region between these two limit cases is difficult to express analytically, but the result of numerical calculation based on Eqs. (7) and (11) is presented in Fig. 2 together with the two curves corresponding to the analytic results in (12) and (13).

Before considering Figs. 2 and 3, we find the crossover area per lipid A^* using the definition

$$\xi(A^*) \equiv Q/2\sqrt{B(A^*)K_f} \approx 1$$

and substituting asymptotic equations (8) and (9) for $B(A^*)$, which both lead to the result

$$A^* = \left(\sqrt{A_0} + \frac{\sqrt{2\pi kT\sqrt{K}}}{Q^{3/4}}\right)^2. \qquad (14)$$

It follows from (14) that as $Q \to 0$, we have $A^* \to \infty$ and, hence, the crossover to the stretching-dominated region of areas per lipid is shifted away from the interval of reasonable areas A: $A \geq A_0$. Therefore, for too small stretching modulus Q, the bending-dominated dependence $P(A)$ derived in (8) occupies the whole A axis and crossover does not occur. It is convenient to evaluate the relative strength of the stretching and bending energies of a chain by a dimensionless parameter $\sigma = QL^2/K_f$. Hence, the bending-dominated isotherm is marked *1* in Fig. 2. In the opposite limit $K \to 0$, it follows from (14) that $A^* \to A_0$, i.e., the whole A axis is occupied by the stretching-dominated region, and the corresponding stretching-dominated isotherm derived in (9) is marked *3* in Fig. 2.

Isotherm *2* in Fig. 2 exhibits the crossover from the bending-dominated region at small areas per lipid, $A \leq A^*$, to the stretching-dominated interval at greater areas, $A \geq A^*$. As follows from Eq. (14), the bending-

dominated region $A_0 \le A \le A^*$ shrinks when the temperature T decreases.

It turns out that more informative than isotherms themselves are the plots of their logarithmic derivatives presented in Fig. 3, $d\ln P_t/d\ln(A-A_0) \approx -\alpha(A)$ vs. A/A_0. This becomes obvious after writing isotherm equations (12) and (13) in the limit $A \to A_0$:

$$P_t \approx \frac{4\pi^{1/3}(k_BT)^{4/3}LA_0^{1/3}}{3K_f^{1/3}}(A-A_0)^{-5/3}, \quad \alpha = 5/3, \quad \xi \ll 1, \tag{15}$$

$$P_t \approx \frac{16\pi(k_BT)^2LA_0}{Q}(A-A_0)^{-3}, \quad \alpha = 3, \quad \xi \gg 1. \tag{16}$$

Hence, by fitting the experimental isotherm of a lipid bilayer with the hyperbolas in Eq. (15) or Eq. (16), it is possible, in principle, to determine which case, $\xi \ll 1$ or $\xi \gg 1$, corresponds to the state of the lipid bilayer. Subsequently, the relevant effective "microscopic" elastic moduli K_f and Q of an individual lipid chain can be deduced using Eqs. (15) and (16), which contain these parameters as prefactors.

5. CHAIN ORDER PARAMETER AND MACROSCOPIC ELASTIC MODULI OF A LIPID BILAYER FROM THE STRING MODEL

To make numerical estimates based on our model of a lipid (bi)layer, Eq. (1), we use the following parameters: chain length $L = 15$ Å, chain incompressible area $A_0 = 20\,\text{Å}^2$, and $T_0 = 300$ K as the reference temperature. The chain flexural rigidity is defined as [27] $K_f = EI$, where $E \approx 0.6$ GPa is the chain Young modulus [28] and $I = A_0^2/4\pi$ is the (geometric) moment of inertia. The flexural rigidity can also be evaluated from the polymer theory [29] as $K_f = k_BTl_p$, where $l_p \approx L/3$ is the chain persistence length [28]. Both estimates approximately give $K_f \approx k_BTL/3$ at the chosen L and $T = T_0$. The value of the stretching modulus Q can be estimated using energy functional (1) and assuming that both contributions due to bending and stretching energies are of the same order; this yields $Q \sim 10^{-6}$–10^{-5} dyn.

Differentiation of $P_t(A)$ gives the area compressibility modulus $K_a = -AdP_t(A,T)/dA$ as a function of the area per chain and temperature. Analytic expressions for this modulus are then derived from Eqs. (12) and (13):

$$K_a = VkT\left(\frac{\pi k_BT}{4K_f}\right)^{1/3} \times \left(A^{-3/2}\left(\sqrt{A}-\sqrt{A_0}\right)^{-5/3} + \frac{5}{9}A^{-1}\left(\sqrt{A}-\sqrt{A_0}\right)^{-8/3}\right), \quad \xi \ll 1, \tag{17}$$

$$K_a = \frac{3\pi V(kT)^2}{Q}\left(A^{-3/2}\left(\sqrt{A}-\sqrt{A_0}\right)^{-3} + A^{-1}\left(\sqrt{A}-\sqrt{A_0}\right)^{-4}\right), \quad \xi \gg 1. \tag{18}$$

Equation (17) is valid in the area interval with dominant bending energy, while Eq. (18) applies to the area interval with dominant stretching energy. When areas per lipid are sufficiently close to A_0, expressions (17) and (18) can be further simplified by retaining only the most diverging terms. In this way, we conclude that under a decrease in the area per lipid A (shrinking of the bilayer), the dependence of the area compressibility modulus on the area per lipid $K_a(A)$ must change from $K_a \sim (A-A_0)^{-4}$ in the stretching-dominated region to $K_a \sim (A-A_0)^{-8/3}$ in the bending-dominated region. The absolute value of the modulus K_a calculated using (18) with other parameters $T = 300$ K, $L = 15\,\text{Å}$, $A_0 = 20\,\text{Å}^2$, $P_{eff} = 100$ dyn/cm, and $Q \approx 10^{-6}$ dyn is $K_a \sim 420$ erg/cm^2. This theoretical value agrees quite well with the known data $K_a \approx 300$ erg/cm^2 [26]. The calculated temperature dependence of the equilibrium area A_t for a fixed value of $\sigma = QL^2/K_f \sim 10^2$ is shown in Fig. 4. From this data, we also find the temperature coefficient of area expansion $K_T = dA_t/A_tdT \approx 0.9 \cdot 10^{-3}$ K^{-1}, in good agreement with the data in [26, 30]: $K_T \sim 10^{-3}$ K^{-1}.

It is also interesting to find how the area compressibility modulus depends on the relative strength of the stretching energy with respect to the bending energy of the lipid chain, which is reflected by the dimensionless parameter $\sigma = QL^2/K_f$ introduced above. Our theoretical results presented in Fig. 5 demonstrate an increase in the area compressibility modulus K_a of the lipid bilayer as a function of σ. However, an increase in K_a by approximately three times necessitates the corresponding increase in the parameter σ by three orders of magnitude. Simultaneously, under such an increase in σ, the equilibrium area per lipid A_t in the layer decreases approximately by a factor of 2, as follows from our results presented in Fig. 6. The curves in Figs. 5 and 6 together may be interpreted as lateral "hardening" of the lipid layer due to shrinking of the average nearest-neighbor interchain distances when stretching

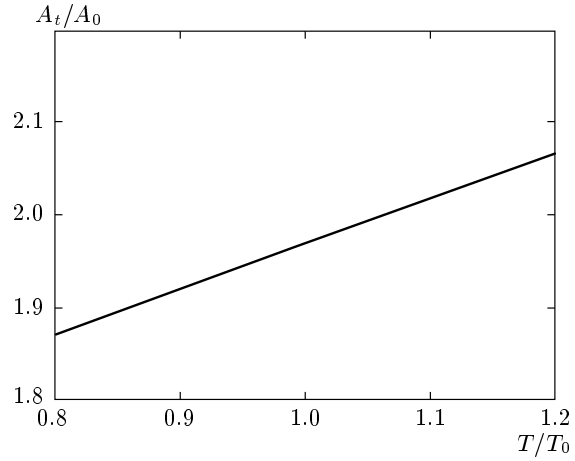

Fig. 4. The calculated temperature dependence of the equilibrium area per lipid A_t in the lipid bilayer for the fixed value $\sigma \sim 10^2$ characterizing the ratio of the chain stretching and bending energies. Other parameters are: $T_0 = 300$ K, $L = 15$ Å, $A_0 = 20$ Å^2, and $P_{eff} = 100$ dyn/cm

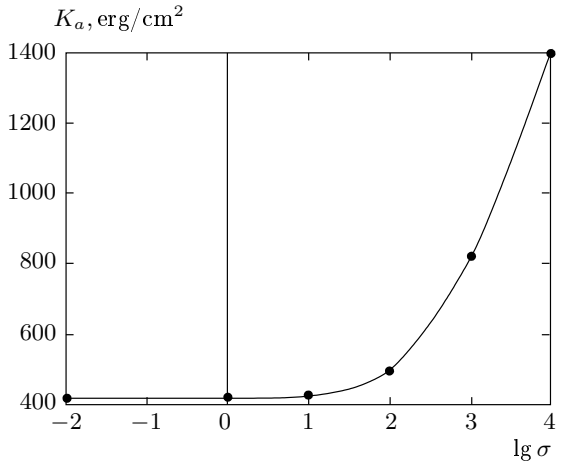

Fig. 5. The calculated area compressibility modulus K_a of the lipid bilayer as a function of the dimensionless parameter $\sigma = QL^2/K_f$. The other parameters are as in Fig. 4. The greater values of σ correspond to the relative strength of the stretching energy of a hydrocarbon chain increasing with respect to its bending energy

energy is added. This is understandable if we realize that the stretching energy makes wiggling of the lipid tails energetically unfavorable. This, in turn, "pushes" the lipid layer closer to a gel-like state with a higher area density of lipids. This semi-intuitive explanation is further supported by our calculations of the chain

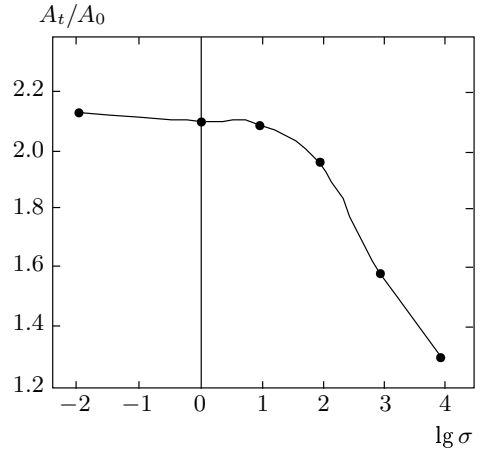

Fig. 6. The calculated equilibrium area per lipid A_t in the lipid bilayer as a function of the dimensionless parameter $\sigma = QL^2/K_f$ characterizing the relative strength of the stretching and bending energies of the individual hydrocarbon chains in the lipid bilayer. The greater values of σ correspond to the relative strength of the stretching energy of a hydrocarbon chain increasing with respect to its bending energy. The other parameters are as in Fig. 4

order parameter

$$S(\theta) = \frac{1}{2}\left(3\langle\cos^2\theta\rangle - 1\right),$$

where the local tangent angle $\theta(z)$ is averaged along the length of the chain $0 \le z \le L$ and the thermodynamic average over different chain conformations is also performed. In calculations, we use the approximate relation valid for small deviations of the chain from the vertical straight line (parallel to the z axis in Fig. 1):

$$1 - \langle\cos^2\theta\rangle \approx \langle \mathrm{tg}^2\,\theta\rangle \propto \langle (X'(z))^2\rangle = \\ = \frac{1}{2\pi}\int\limits_{-\pi/a}^{\pi/a} \frac{q^2 T}{E_q}\, dq. \quad (19)$$

Because the order parameter is in the range $0 \le S(\theta) \le 1$, the approximate relation in Eq. (19) is valid as long as deviations of the chains from the straight line are small:

$$\theta \sim \frac{\sqrt{\langle X^2(z)\rangle}}{L} \ll 1.$$

Thus, besides being an important characteristic of the prevailing conformations of the chains in the lipid bilayer, the order parameter provides a consistency check. The results of calculations are presented in Fig. 7. It

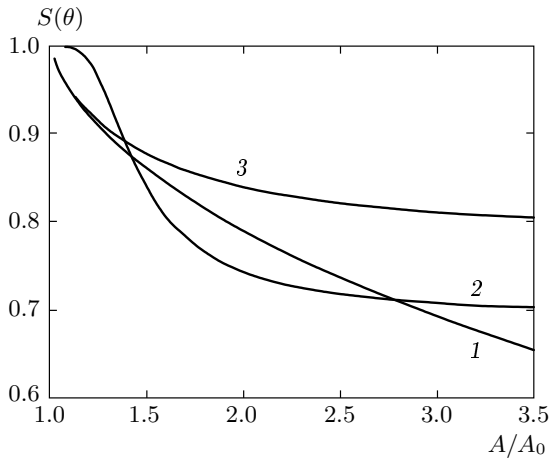

Fig. 7. The calculated chain order parameter $S(\theta) = 1/2\left(3\langle\cos^2\theta\rangle - 1\right)$ as a function of the area per lipid in a lipid (bi)layer. A_0 is the incompressible area of the hydrocarbon chain. The local tangent angle $\theta(z)$ is averaged over the length of the chain $0 \le z \le L$ and over different chain conformations. Curve *1* ($S_K(\theta)$, $\sigma \to 0$) corresponds to the dominant bending energy of the chains; curve *2* ($S_Q(\theta)$, $\sigma \to \infty$) corresponds to the dominant stretching energy of the chains; curve *3* ($S_\sum(\theta)$, $\sigma \approx 10^2$) corresponds to an intermediate case and shows a crossover between the curves drawn in the two limits mentioned above. The other parameters are as in Fig. 4

is easier to understand the origin of the different limit curves in Fig. 7 when Eq. (19) is rewritten using the definition given after Eq. (3):

$$E_q = K_f q^4 + Qq^2 + B. \tag{20}$$

Then, in the limit as $\sigma \to 0$, when bending energy dominates, the term proportional to q^2 in E_q vanishes. Simultaneously, due to the bending energy contribution ($\sim K_f q^4$), the integral in Eq. (19) converges at small wave vectors $q \le (B(A)/K_f)^{1/4}$, leading to a decrease in the order parameter with increasing the area per lipid:

$$S(\theta) \approx 1 - \text{const}\,(B(A))^{-1/4},$$

where $B(A) \sim (A - A_0)^{-8/3}$ in accordance with Eq. (8). In the opposite limit $\sigma \to \infty$, when stretching energy dominates, we obtain the following expression for the integral in Eq. (19):

$$\langle (X'(z))^2\rangle = \frac{1}{2\pi}\int\limits_{-\pi/a}^{\pi/a} \frac{q^2 dq}{Qq^2 + B(A)} =$$

$$= \frac{T}{aQ}\left(1 - \sqrt{\frac{B}{Q}}\,\frac{L}{N\pi}\,\text{arctg}\left(\sqrt{\frac{Q}{B}}\,\frac{N\pi}{L}\right)\right). \tag{21}$$

Hence, in the limit $\sqrt{B(A)/Q}L/N\pi \gg 1$, i.e., as $A \to A_0$, we find $\langle (X')^2\rangle \to 0$, and therefore $S(\theta)_{\sigma\to\infty} \to 1$. In the opposite limit $\sqrt{B(A)/Q}L/N\pi \ll 1$, i.e., when A sufficiently exceeds A_0, $\langle (X')^2\rangle \approx NT/LQ$, and hence the order parameter is practically area-independent, $S(\theta)_{\sigma\to\infty} \approx \text{const} < 1$, as seen in Fig. 7, where $S(\theta)_{\sigma\to\infty} \equiv S_Q$ becomes flat as A/A_0 increases. In the intermediate case (see curve *3*), the order parameter as a function of the area per lipid interpolates qualitatively between the two limit dependences just described.

Finally, we observe that as follows from Fig. 7, our approximation of small deviations of the chain from a straight line is valid with the chosen numerical values of the basic parameters of the lipids up to areas per lipid $A/A_0 \le 3$, because the deviation of the order parameter $S(\theta)$ from 1 in all the considered regimes turns out to be small: $1 - S(\theta) \le 0.3$.

6. CONCLUSIONS

We derived analytic expressions for the pressure–area isotherms of a lipid bilayer using the string model of hydrocarbon chains that includes flexural and stretching moduli of a single chain and the self-consistent entropic repulsion acting between the chains in the lipid bilayer. A crossover on the pressure–area isotherm is predicted to arise due to the competition between bending and stretching contributions to the total conformational energy of the individual chains. A theoretical method of the data analysis is proposed that in principle permits deducing the microscopic effective elastic moduli of the individual lipid molecules by studying pressure–area isotherms of the macroscopic lipid (bi)layer. The applicability criteria and checks of the theory using comparison with known experimental and numerical simulation data for lipid bilayers are presented. A generalization of the proposed model to the description of spatially inhomogeneous thermodynamic states of lipid bilayers is in progress.

The authors are grateful to M. Deserno for his useful comments on the preprint of this work.

REFERENCES

1. R. S. Cantor, Biophys. J. **76**, 2625 (1999).
2. D. Marsh, Biochim. Biophys. Acta **1286**, 183 (1996).
3. S. I. Sukharev, W. J. Sigurdson, C. Kung et al., J. Gen. Physiol. **113**, 525 (1999).
4. A. Ben-Shaul, *Structure and Dynamics of Membranes*, Elsevier, Amsterdam (1995).
5. A. F. Mingotaud, C. Mingotaud, and L. K. Patterson, *Handbook of Monolayers*, Academic, San Diego (1993).
6. Ping Sheng, Phys. Rev. Lett. **37**, 1059 (1976).
7. J. N. Israelachvili, Langmuir **10**, 3774 (1994).
8. E. Ruckenstein and B. Li, Langmuir **12**, 2308 (1996).
9. E. Ruckenstein and B. Li, J. Phys. Chem. **102**, 981 (1998).
10. P. I. Kuzmin, S. A. Akimov, Yu. A. Chizmadzhev, J. Zimmerberg, and F. S. Cohen, Biophys. J. **88**, 1120 (2005).
11. J. L. Harden, F. C. MacKintosh, and P. D. Olmsted, Phys. Rev. E **72**, 011903 (2005).
12. A. J. Kox, J. P. J. Michels, and F. W. Wiegel, Nature (London) **287**, 317 (1980).
13. A. Georgallas and D. A. Pink, J. Colloid Interf. Sci. **62**, 125 (1977).
14. S. Marcelja, Biochim. Biophys. Acta **367**, 165 (1974).
15. J. F. Nagle, J. Membrane Biol. **27**, 233 (1976).
16. A. Caille, D. A. Pink, F. De Verteuil, and M. J. Zuckermann, Canad. J. Phys. **58**, 581 (1980).
17. S. Doniach, J. Chem. Phys. **68**, 4912 (1978).
18. A. Caille, A. Rapini, M. J. Zuckermann, A. Cros, and S. Doniach, Canad. J. Phys. **56**, 348 (1978).
19. F. Jahnig, J. Chem. Phys. **70**, 3279 (1979).
20. R. S. Cantor and K. A. Dill, Langmuir **2**, 231 (1986).
21. J.-L. Firpo, J. J. Dupin, G. Albinet, A. Bois et al., J. Chem. Phys. **68**, 1369 (1978).
22. J. J. Dupin, J.-L. Firpo, G. Albinet, A. Bois et al., J. Chem. Phys. **70**, 2357 (1979).
23. S. I. Mukhin and S. Baoukina, Phys. Rev. E **71**, 061918 (2005).
24. I. N. Krivonos and S. I. Mukhin, Biophys. J. **92**(1) Part 2 Suppl., 583a (2007).
25. W. Rawicz, K. C. Olbrich, T. McIntosh, D. Needham, and E. Evans, Biophys. J. **79**, 328 (2000).
26. E. Lindahl and O. Edholm, J. Chem. Phys. **113**, 3882 (2000).
27. Л. Д. Ландау, Е. М. Лифшиц, *Теория упругости*, т. 7, Наука, Москва (1987).
28. *Энциклопедия полимеров*, Изд-во БСЭ, Москва (1977).
29. D. Nelson, *Defects and Geometry in Condensed Matter Physics*, Cambridge Univ. Press, Cambridge (2002).
30. R. Waugh and E. A. Evans, Biophys. J. **26**, 115 (1979).